Nitrogen-doped carbon nanotubes as cathode for lithium–air batteries

Yongliang Li, Jiajun Wang, Xifei Li, Jian Liu, Dongsheng Geng, Jinli Yang, Ruying Li, Xueliang Sun *

Department of Mechanical and Materials Engineering, University of Western Ontario, 1151 Richmond Street N., London, Ontario, Canada N6A 5B9

ARTICLE INFO

ABSTRACT

Nitrogen-doped carbon nanotubes (N-CNTs) were synthesized by a floating catalyst chemical vapor deposition (FCCVD) method. Various techniques including X-ray photoelectron spectroscopy, field emission scanning electron microscopy, transmission electron microscopy, X-ray diffraction, and Raman spectroscopy revealed the morphology and structure of CNTs and N-CNTs as well confirmed the existence of incorporated nitrogen (10.2 at.%) in N-CNTs. N-CNTs were investigated as cathode material for lithium–air batteries and exhibited a specific discharge capacity of 866 mAh g^{-1}, which was about 1.5 times as that of CNTs. Our results indicated that the N-CNTs electrode showed high electrocatalytic activities for the cathode reaction thus improving the lithium–air battery performance.

© 2011 Elsevier B.V. All rights reserved.

1. Introduction

Lithium–air batteries have been attracting much attention due to its extremely high theoretical specific energy [1]. The cathode active material, oxygen, is not stored in the batteries, but can be absorbed from the environment during discharge, making these systems serious contenders to meet the rapid growing requirements of the hybrid electric vehicles (HEVs) and electric vehicles (EVs) [2]. Many work indicated that the battery performance strongly depended on the carbon cathode [3–5]. For example, Xiao et al. found that the surface area and mesopore volume of carbon powder significantly affected the discharge capacity [6]. Mirzaeian et al. found that the battery performance depended on the morphology of the carbon as well [7]. Therefore it is important to develop new carbon-based electrodes to improve the kinetics of the air cathode and to enhance the battery performance.

Recently, nitrogen-doped carbon powder as cathode material in lithium–air batteries showed improvement to the discharge capacity because of the high surface area, porosity and electrocatalytic activity [8]. The doped heteroatoms are available to tailor the chemical and electronic nature of carbon-based materials [9–11]. Recent work has shown that the N-CNTs exhibited excellent electrocatalytic activity for oxygen reduction reaction (ORR) in aqueous electrolyte [12–15]. Zhang et al. reported that the battery made with carbon nanotube/nanofiber mixed buckpapers cathode delivered a high discharge capacity [16]. However, to our best knowledge, no research on N-CNTs as cathode for lithium–air batteries was reported.

In this work, for the first time, we employed N-CNTs as cathode for lithium–air batteries. It was demonstrated that nitrogen doping into carbon nanotubes not only increased the discharge capacity but also enhanced the reversibility in the charge/discharge process. This finding is opening a rational and promising direction in developing carbon electrode for lithium–air batteries.

2. Experimental

2.1. Materials synthesis

CNTs with diameters of 40–60 nm were purchased from Shenzhen Nanotech., China. N-CNTs were prepared in our group by a floating catalyst chemical vapor deposition (FCCVD) method, as described before [11]. Imidazole was used as carbon and nitrogen source, and ferrocene as catalyst precursor. At 850 °C, ferrocene decomposed into iron as the catalyst for carbon nanotube growth and the nitrogen atoms incorporated into the graphite layers to yield N-CNTs.

2.2. Physical characterizations

The morphologies and structures of CNTs and N-CNTs were characterized by a Hitachi S-4800 field emission scanning electron microscopy (FESEM) and a Hitachi H-7000 transmission electron microscopy (TEM). Powder X-ray diffraction (XRD) patterns were recorded by a Rigaku RU-200BVH diffractometer employing a Co-Kα source (λ = 1.7892 Å). Raman scattering (RS) spectra were recorded on a HORIBA Scientific LabRAM HR Raman spectrometer system equipped with a 532.4 nm laser. N$_2$ adsorption/desorption isotherms were obtained using a Folio Micromeritics TriStar II Surface Area and Pore

* Corresponding author. Tel.: +1 519 6612111x87759; fax: +1 519 6613020.
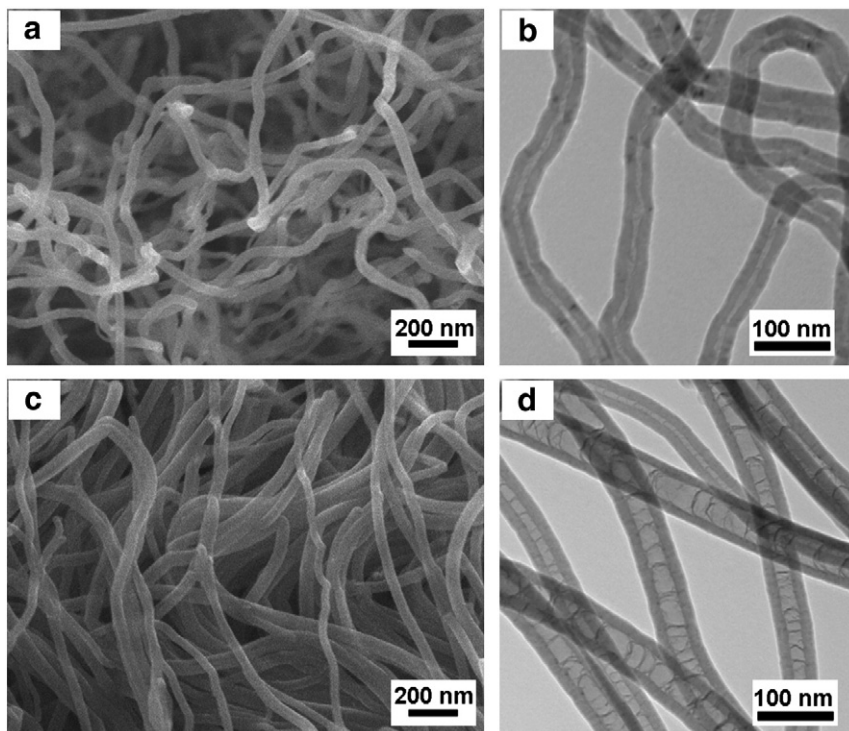*E-mail address:* xsun@eng.uwo.ca (X. Sun).

Fig. 1. SEM and TEM images of CNTs (a, and b) and N-CNTs (c, and d).
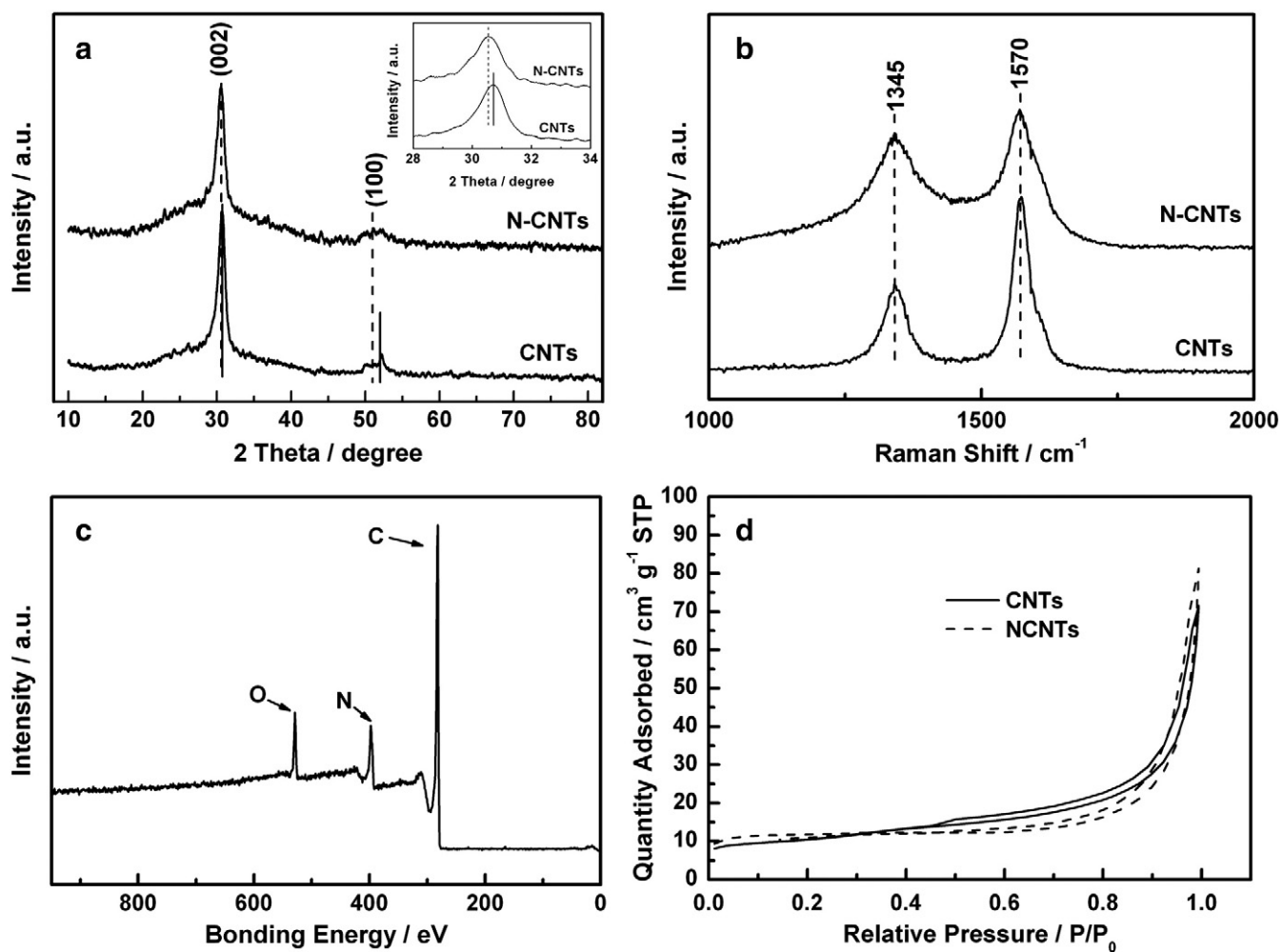

Fig. 2. (a) XRD patterns of the CNTs and N-CNTs, (b) Raman spectra of the CNTs and N-CNTs, (c) XPS survey spectrum of the N-CNTs, and (d) N_2 adsorption–desorption isotherms for the CNTs and N-CNTs. The inset of a is the XRD patterns in the range between 28° and 34°.
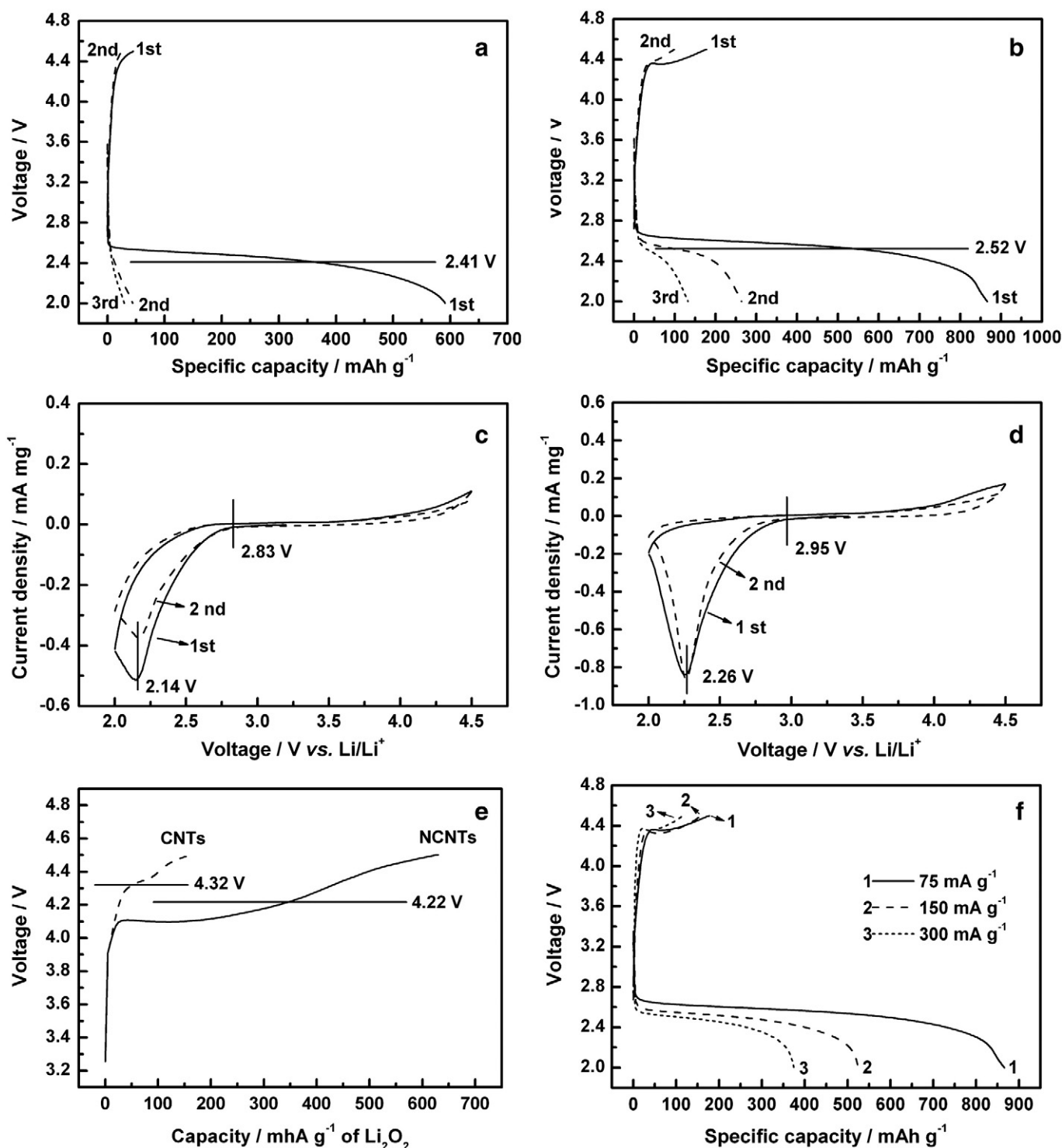
Fig. 3. The voltage profiles of (a) CNTs and (b) N-CNTs electrodes cycled in a voltage range of 2.0–4.5 V at a current density of 75 mA g^{-1} in the first three cycles; CV curves of (c) CNTs and (d) N-CNTs electrodes in 1 mol LiPF$_6$ in PC:EC (1:1 wt.%) in 1 atm O$_2$ at 25 °C at a scan rate of 0.2 mV s^{-1}; (e) Variation of Voltage on charging cells with CNTs and N-CNTs electrodes at a density of 75 mA g^{-1}. Cathode composition: CNTs or N-CNTs/Li$_2$O$_2$/binder (70/20/10); (f) Voltage profiles of N-CNTs electrodes at current densities of 75, 150, and 300 mA g^{-1}.

Size Analyser. The nitrogen content in N-CNTs was determined by a Kratos Axis Ultra X-ray photoelectron spectrometer with Al Kα as the X-ray source.

2.3. Electrochemical measurements

Cathode was prepared by casting a mixture of CNTs (or N-CNTs), and PVDF (Alfa Aesar) with a weight ratio of 9:1 onto a separator (Celgard 3500). The electrode is 3/8 in in diameter and the carbon loadings were 0.5 ± 0.1 mg. The electrolyte was 1 mol LiPF$_6$ (Sigma Aldrich, 99.99%) dissolved in propylene carbonate (PC) (Sigma Aldrich, anhydrous, 99.7%)/ethylene carbonate (EC) (Alfa Aesar, anhydrous, 99%) (1:1 weight ratio).

Swagelok cells composed of lithium foil, Celgard 3500 separator, different cathodes and stainless steel (SS) mesh as current collector were assembled in an argon-filled glove box (MBraun Inc.) with the

moisture and oxygen concentration <1 ppm. The cells were gastight except for the SS mesh window which exposed to a 1 atm O_2 atmosphere. The discharge/charge characteristics were performed by using an Arbin BT-2000 battery station in a voltage range of 2.0–4.5 V. Cyclic voltammetry measurements were carried out by using a CHI 600c electrochemical work station at a scan rate of 0.2 mV s^{-1} in a voltage range of 2.0–4.5 V at room temperature.

To study the catalytic activity of CNTs and N-CNTs on the charge decomposition of Li_2O_2, the cathode was constructed by using the method previously reported [17]. The cathode was made by casting a mixture of CNTs or N-CNTs, Li_2O_2 (Alfa Aesar), and PVDF at a weight ratio of 7:2:1 onto a Celgard separator. The electrodes were incorporated into Swagelok cells and charged at a current density of 75 mA g^{-1} (of carbon) at room temperature.

3. Results and discussion

Fig. 1 shows SEM and TEM images of CNTs and N-CNTs. Both samples have uniform distributions in diameters (Fig. 1a,c). As shown in Fig. 1b and d, the diameter of CNTs is about 40–50 nm, while for N-CNTs is about 50–60 nm. The typical bamboo-like structure in N-CNTs indicates that nitrogen atoms were introduced into the carbon network [11].

XRD patterns of CNTs and N-CNTs are shown in Fig. 2a. The diffraction peaks at around 30° and 52° correspond to the (002) and (100) facets of hexagonal graphitic carbon, respectively. However, the diffraction peaks of N-CNTs slightly shifted to lower 2θ values than those of CNTs, which is due to the distortion in the graphene layers resulting from the incorporation of nitrogen [18].

Fig. 2b shows the Raman spectra of CNTs and N-CNTs. Both samples exhibit two obvious peaks at ~1345 and ~1570 cm^{-1}, corresponding to the D and G bands, respectively. The D band denotes the disordered graphite structure, whereas the G band indicates the presence of crystalline graphitic carbon. The intensity ratio of D and G bands (I_D/I_G) is used to evaluate the disorder in the materials [19]. The I_D/I_G ratios of CNTs and N-CNTs are 0.53 and 0.85, respectively. The higher I_D/I_G ratio implies more defects in N-CNTs.

The XPS survey spectrum is shown in Fig. 2c. Three strong peaks at 282, 398, and 529 eV are attributed to C1s, N1s and O1s, respectively. The atomic concentration of N can be estimated by the peak area ratio between N and C + N [20]. The nitrogen content in the as-prepared N-CNTs is ca. 10.2 at.%.

The N_2 adsorption–desorption isotherms for the CNTs and N-CNTs are shown in Fig. 2d. Both samples are found to yield type-I isotherm, which indicates the presence of micropores and mesopores [21]. The BET surface area and total pore volume for CNTs are 44.95 m^{2}g^{-1} and 0.081 cm^{3}g^{-1} while for N-CNTs are 40.92 m^{2}g^{-1} and 0.073 cm^{3}g^{-1}, respectively. The differences are due to the different diameters, but both samples have similar pore size, ~7.3 nm.

As shown in Fig. 3a and b, the N-CNTs deliver an initial discharge capacity of 866 mAh g^{-1}, while 590 mAh g^{-1} for CNTs. Clearly, N-CNTs show a capacity about 1.5 times as that of the CNTs, although N-CNTs have lower BET surface area and pore volume [6]. The high specific capacity results from the electrocatalytic activity of N-CNTs itself which facilitates the cathode reactions during discharge [8]. The discharge average voltage plateau of N-CNTs is ~2.52 V, which is higher than that of CNTs, ~2.41 V. The voltage difference, ~0.1 V, between the N-CNTs and CNTs electrode remains through the whole discharge process, indicating a higher ORR activity on the N-CNTs electrode. To further compare the catalytic activity of the electrodes, cyclic voltammetry measurements were conducted. It can be seen from the CV curves in Fig. 3c and d that the onset voltage and peak voltage of N-CNTs are ~2.95 V and ~2.26 V, while for CNTs are ~2.83 V and ~2.14 V, respectively, which is consistent with the results in Fig. 3a,b.

It is noticed that the discharge capacities of the second and the third cycles of N-CNTs are 264 and 133 mAh g^{-1}, respectively, whereas the capacities of CNTs electrode drop dramatically to less than 45 mAh g^{-1} in the second and the third cycles, therefore CNTs cathode shows limited reversibility (Fig. 3a,b). In order to compare the reversibility of CNTs and N-CNTs, their charge behavior for the electrochemical decomposition of the discharge product, Li_2O_2, is shown in Fig. 3e. The N-CNTs have lower average charging plateau voltage (4.22 V) and higher capacity (630 mAh g^{-1} of Li_2O_2) than CNTs. These results reveal that the N-CNTs are more efficient for Li_2O_2 decomposition, indicating a high catalytic activity in the charge process. The discharge capacities of N-CNTs electrode at different current densities are shown in Fig. 3f. With the increase of the current densities, the discharge capacities decreases, 866, 525, and 374 mAh g^{-1} at current densities of 75, 150, and 300 mA g^{-1}, respectively. This is because the electrochemical polarization becomes much more significant at high current densities [22].

The role of nitrogen doping in the CNTs for the electrocatalytic activities in lithium–air batteries is not clear now, and the understanding about the catalytic behavior of N-CNTs for ORR in nonaqueous electrolyte is scarce to date. Maybe the doped-nitrogen with lone electron pair could provide additional negative charges which enhance the interaction between carbon structures and foreign molecules and increase the conductivity, thus improves the electrode reactions for lithium–air batteries [14,15,23,24]. The related work is carrying out in our group to understand the doping effect.

4. Conclusions

The electrochemical performance of CNTs and N-CNTs electrodes was studied in lithium–air batteries. The N-CNTs electrode has a specific discharge capacity of 866 mAh g^{-1}, which is about 1.5 times as that of CNTs. It was demonstrated the N-CNTs have much better electrocatalytic activity for Li_2O_2 decomposition, therefore, improving the reversibility for lithium–air batteries. The performance improvement of N-CNTs results from heteroatom nitrogen doping. The detailed fundamental mechanism is under study.

Acknowledgements

References

[1] K.M. Abraham, Z. Jiang, J. Electrochem. Soc. 143 (1996) 1.
[2] G. Girishkumar, B. McCloskey, A.C. Luntz, S. Swanson, W. Wilcke, J. Phys. Chem. Lett. 1 (2010) 2193.
[3] A. Débart, J. Bao, G. Armstrong, P.G. Bruce, J. Power Sources 174 (2007) 1177.
[4] J. Read, J. Electrochem. Soc. 149 (2002) A1190.
[5] Y. Lu, H.A. Gasteiger, M.C. Parent, V. Chiloyan, S.-H. Yang, Electrochem. Solid State Lett. 13 (2010) A69.
[6] J. Xiao, D. Wang, W. Xu, D. Wang, R.E. Williford, J. Liu, J. Zhang, J. Electrochem. Soc. 157 (2010) A487.
[7] M. Mirzaeian, P.J. Hall, Electrochim. Acta 54 (2009) 7444.
[8] P. Kichambare, J. Kumar, S. Rodrigues, B. Kumar, J. Power Sources 196 (2011) 3310.
[9] D. Geng, H. Liu, Y. Chen, R. Li, X. Sun, S. Ye, S. Knights, J. Power Sources 196 (2010) 1795.
[10] Y. Chen, J. Wang, H. Liu, M. Banis, R. Li, X. Sun, T. Sham, S. Ye, S. Knights, J. Phys. Chem. C 115 (2011) 3769.
[11] H. Liu, Y. Zhang, R. Li, X. Sun, S. Desilets, H. Abou-Rachid, M. Jaidann, L.-S. Lussier, Carbon 48 (2010) 1498.
[12] K. Gong, F. Du, Z. Xia, M. Durstock, L. Dai, Science 323 (2009) 760.
[13] W. Xiong, F. Du, Y. Liu, A. Perez Jr., M. Supp, T.S. Ramakrishnan, L. Dai, L. Jiang, J. Am. Chem. Soc. 132 (2010) 15839.
[14] M. Saha, R. Li, X. Sun, S. Ye, S. Knights, Electrochem. Commun. 11 (2009) 438.
[15] Y. Chen, J. Wang, H. Liu, R. Li, X. Sun, S. Ye, S. Knights, Electrochem. Commun. 11 (2009) 2071.
[16] G.Q. Zhang, J.P. Zheng, R. Liang, C. Zhang, B. Wang, M. Hendrickson, E.J. Plichta, J. Electrochem. Soc. 157 (2010) A953.

[17] V. Giordani, S.A. Freunberger, P.G. Bruce, J.-M. Tarascon, D. Larcher, Electrochem. Solid State Lett. 13 (2010) A180.
[18] S. Lim, S. Yoon, I. Mochida, D. Jung, Langmuir 25 (2009) 8268.
[19] J.H. Huang, W.J. Chen, C.C. Lee, Y.Y. Chang, Diamond Relat. Mater. 13 (2004) 1012.
[20] M. Nath, B.C. Satishkumar, A. Govindaraj, C.P. Vinod, C. Rao, Chem. Phys. Lett. 322 (2000) 333.
[21] Y. Fang, D. Gu, Y. Zou, Z.X. Wu, F.Y. Li, R.C. Che, Y.H. Deng, B. Tu, D.Y. Zhao, Angew. Chem. Int. Ed. 49 (2010) 7987.
[22] S.S. Zhang, D. Foster, J. Read, J. Power Sources 195 (2010) 1235.
[23] P. Ayala, R. Arenal, M. Rümmeli, A. Rubio, T. Pichler, Carbon 48 (2010) 575.
[24] Y.F. Tang, B.L. Allen, D.R. Kauffman, A. Star, J. Am. Chem. Soc. 131 (2009) 13200.